Biochemical Pharmacology 80 (2010) 1718–1726

Contents lists available at ScienceDirect

Biochemical Pharmacology

journal homepage: www.elsevier.com/locate/biochempharm

Triplex forming oligonucleotides against type α1(I) collagen attenuates liver fibrosis induced by bile duct ligation

Ravikiran Panakanti [a], Akshay Pratap [b], Ningning Yang [a], John S. Jackson [c], Ram I. Mahato [a,*]

[a] Department of Pharmaceutical Sciences, University of Tennessee Health Science Center, Memphis, TN 38103, USA
[b] Division of Solid Organ Transplantation, Methodist University Hospital Transplant Institute, Memphis, TN 38104, USA
[c] Department of Comparative Medicine, University of Tennessee Health Science Center, Memphis, TN 38163, USA

ARTICLE INFO

Article history:
Received 29 June 2010
Accepted 25 August 2010

Keywords:
Liver fibrosis
Triplex forming oligonucleotide
Common bile duct ligation
Type α1(I) collagen
TGF-β1
α-SMA

ABSTRACT

Liver fibrosis is a consequence of chronic liver disorders which lead to the accumulation of extracellular matrix (ECM). Particularly, there is an increased accumulation of collagen in the fibrotic liver. We have therefore used a triplex forming oligonucleotide (TFO) against the type α1(I) collagen and evaluated, whether it can attenuate liver fibrosis induced by common bile duct ligation (CBDL) in rats. There was a significant decrease in hydroxyproline levels and Masson's trichrome staining for collagen in TFO-treated CBDL groups compared to non-treated CBDL group. There was over expression of type α1(I) collagen, α-smooth muscle actin (α-SMA) and TGF-β1 expression in the CBDL group compared to TFO-treated CBDL group. Also, the serum alanine transaminase (ALT) and aspartate transaminase (AST) concentrations were less in the TFO treated group compared to non-treated CBDL group. There was also less neutrophils accumulation in TFO treated CBDL group assayed by myeloperoxidase (MPO) assay. These results suggests that TFO can be used to downregulate type 1 collagen gene expression and can alleviate liver fibrosis induced by common bile duct ligation.

1. Introduction

Liver fibrosis results from chronic damage to the liver in conjunction with the accumulation of extracellular matrix (ECM) proteins, which is a characteristic of most chronic liver diseases [1]. The main causes of liver fibrosis in industrialized countries include chronic hepatitis C virus (HCV) infection, alcohol abuse, and nonalcoholic steatohepatitis (NASH). Such chronic diseases lead to scarring formation in the liver that, with increasing severity, prevention of effective liver regeneration and maintenance of liver function [2]. Liver fibrosis is associated with major alterations in both the quantity and composition of ECM. The accumulation of ECM proteins distorts the hepatic architecture by forming a fibrous scar, and the subsequent development of nodules of regenerating hepatocytes defines cirrhosis [3].

Type I collagen, the major component of the extracellular matrix in the fibrotic liver, is a heterotrimer composed of 2α1 chains and 1α2 chain. These chains are encoded by two distinct genes, COLlAl and COLlA2, respectively. Hepatic stellate cells (HSCs; also known as vitamin A-storing cells, fat-storing cells, Ito cells, and lipocytes) residing in the perisinusoidal space of Disse in the liver, are the main producers of type α1(I) collagen and other components of extracellular matrix in both normal and fibrotic livers [4,5]. Following chronic injury, cytokines such as transforming growth factor β (TGF-β) and protein kinase signaling pathways mediate a complex interplay among different hepatic cells [6–8]. Under the influence of these signals, HSCs activate or transdifferentiate into myofibroblast-like cells, acquiring contractile, proinflammatory, and fibrogenic properties resulting in increased synthesis of types I and III fibrillar collagen [9,10].

In contrast with the traditional view that cirrhosis is an irreversible disease, recent evidence indicates that even advanced fibrosis is reversible [11,12]. Preclinical studies have reported a scientific rationale and experimental evidence supporting the use of many potential therapies for fibrosis. Such therapies have been targeted to any of several different biological targets (e.g., inhibition of collagen synthesis, interruption of matrix deposition, stimulation of matrix degradation, modulation of stellate cell activation, or induction of HSC death). Triplex-forming oligonucleotides (TFOs) constitute an interesting DNA sequence-specific tool that can be used to target cleaving or cross-linking agents, transcription factors or nucleases to a chosen site on the DNA. TFOs have proved effective in altering gene expression by interfering either with the binding of transcription factors [13,14]. Because liver fibrosis is due to the overproduction of type I collagen by liver

* Corresponding author at: Department of Pharmaceutical Sciences, University of Tennessee Health Science Center, 19 S Manassas, RM 224, Memphis, TN 38103-3308, USA. Tel.: +1 901 448 6929; fax: +1 901 448 2099.
E-mail address: rmahato@uthsc.edu (R.I. Mahato).
URL: http://www.uthsc.edu/pharmacy/rmahato

0006-2952/$ – see front matter © 2010 Elsevier Inc. All rights reserved.
doi:10.1016/j.bcp.2010.08.020

fibrogenic cells, targeted inhibition of transcription of type α(I) collagen gene is expected to prevent fibrosis. Recently, we showed that antiparallel phosphorothioate (APS) TFOs specific for α1(1) collagen form triplexes efficiently and inhibit transcription in cultured immortalized rat hepatic stellate cells (HSC-T6) *in vitro* [15]. These results suggest that targeting collagen transcription may theoretically attenuate fibrosis in livers undergoing tissue remodeling.

In the current study, we studied the antifibrotic effects of TFOs in rats undergoing common bile duct ligation (CBDL). TFO administration in CBDL rats resulted in decreased liver injury, inflammation, and fibrosis. At the cellular level, TFO induced similar effects in primary rat HSCs. This evidence indicates that the prevention of fibrosis by anti-collagen TFO treatment could preserve organ function and be therapeutically useful. Our data may suggest that anticollagen TFOs could be effective in future gene therapy for fibrosis in vital organs.

2. Materials and methods

2.1. Materials

TFO, which was a 25-mer antiparallel fully phosphorothioate ODN (3′-GAGGGGGGAGGAGGGAAAGGAAGGG-5′) targeting rat α1(I) collagen gene promoter was synthesized by Invitrogen (Carlsbad, CA). Bovine serum albumin (BSA) (fraction V, purity >98%) was purchased from USB Corporation (Cleveland, OH). SYBR Green-1 dye universal master mix and MultiScribe reverse transcriptase were purchased from Applied Biosystems, Inc. (Foster City, CA). Tumor necrosis factor (TNF)-α ELISA kits were purchased from eBioscience, Inc. (San Diego, CA). RNA extraction kit was procured from Promega (Madison, WI). Immobilon polyvinylidene fluoride (PVDF) membrane was purchased from Millipore (Billerica, MA). Rabbit antirat TGF-β1 and β-actin primary antibodies and horseradish peroxidase-conjugated goat antirabbit secondary antibody were purchased from Santa Cruz Biotechnology (Santa Cruz, CA). Chemiluminescence (ECL) detection kit was purchased from GE Healthcare Life Sciences (Pittsburgh, PA). Serum alanine transaminase and aspartate transaminase kits were purchased from ID Labs, Inc (London, Canada). Citric acid and sodium citrate were procured from Curtin Matheson Scientific, Inc (Houston, TX). Sodium hydroxide was purchased from Fisher Scientific, (Fair Lawn, NJ). Hydroxyproline, Chloramine-T, 3,3′-diaminobenzidine (DAB) and goat serum were purchased from Sigma-Aldrich (St. Louis, MO).

2.2. Animals and experimental design

Male Sprague–Dawley rats weighing 250–280 g were maintained under conditions as per the NIH (http://grants1.nih.gov/grants/olaw/references/phspol.htm) and institutional animal care and use Committee using the approved protocol. All animals were housed in microisolator cages in virus-free facilities and fed laboratory chow *ad libitum*. Common bile duct ligation (CBDL) or sham operation was performed as described previously [16–18]. After a midline laparotomy, liver lobes were retracted upwards and the intestines were reflected to the right to expose the common bile duct (CBD). The CBD was then isolated by careful blunt dissection, doubly ligated with 4-0 silk and transected between the two ligations. The sham operation was performed similarly, with the exception of ligating and transecting the bile duct. Liver was then replaced into the abdominal cavity making sure there were no twists in the vascular pedicles of its lobes. The abdomen was closed with 4-0 silk running suture. Rats were injected with TFO at 8 mg/kg per dose twice a week for 4 weeks via the tail vein. Sham operated rats and CBDL control rats were injected with an equal volume of saline. Animals were sacrificed after 7 weeks. Blood and liver tissue were collected for biochemical, RNA, histological and Immunohistochemical studies.

2.3. Cell culture

Immortalized rat hepatic stellate cells (HSC-T6) were a kind gift by Dr. Scott Friedman (Mount Sinai School of Medicine, New York). HSC-T6 cells at a density of 1×10^6 cells were seeded on uncoated plastic tissue culture 6-well plates and cultured in Dulbecco's Modified Eagle Medium (DMEM, Gibco BRL, Grand Island, NY) containing 10% of fetal bovine serum (FBS) until 50% confluence was achieved. The growth medium was replaced with a pre-warmed serum-free DMEM. TFO was mixed with lipofectamine 2000 according to the manufacture's protocol and then used for transfection.

2.4. Serum transaminase levels

Serum levels of aspartate aminotransferase (AST) and alanine aminotransferase (ALT) were used as markers of liver injury. ALT and AST concentrations were measured using IDTox™ Alanine Transaminase color endpoint assay kit and IDTox™ Aspartate Transaminase (AST) Enzyme Assay Kit (ID Labs™ Inc, London, ON, Canada) according to the manufacturer's instructions and absorbance was measured using a spectrophotometer.

2.5. Hydroxyproline assay

Hydroxyproline content was quantified colorimetrically from 30 mg of liver tissue as previously described [19]. Briefly, fresh liver tissue was collected and weighed at the time of sacrificing the animals. The tissue was then hydrolyzed with 6N HCl and then heated in an oven at 110 °C for 18 h. The tissue was incubated in a vacuum desiccator overnight until the HCl was completely dried. Citrate buffer was added to dilute the samples, Chloramine-T reagent added to the samples and allowed to react for 20 min at room temperature. Following this, fresh Ehrlich's reagent (manufacture name) was prepared and added to each sample. Samples were then placed in a warm water bath (60 °C) and allowed to react for 15 min. Samples were then cooled to room temperature and absorbance was read at 550 nm for each sample and a standard control. The results were expressed as micrograms of hydroxyproline per grams of liver.

2.6. ELISA for tumor necrosis factor-α

Cell culture supernatant or serum was used to determine the levels of TNF-α using an ELISA kit according to the manufacturer's specifications (eBiosciences, San Diego, CA). For *in vitro* studies, rat HSC-T6 cells were cultured as described above. Medium was removed and cells incubated in serum-free medium for 24 h. Supernatants were collected and stored at −80 °C until analysis. For *in vivo* studies, blood was collected immediately after euthanasia and centrifuged at 10,000 rpm for 7 min at room temperature to separate the serum. Serum was at −80 °C for future use. ELISA data were then presented as the percentage (%) of the control for *in vitro* studies or picograms per milliliter of serum for *in vivo* studies.

2.7. Real-time polymerase chain reaction

To determine type I collagen, alpha smooth muscle actin (α-SMA), TGF-β1, and tissue inhibitor of metalloproteinase 1 (TIMP-1) gene expression in rat liver, total liver RNA was extracted using

RNeasy extraction kit (Qiagen, Valencia, CA). RNA concentration and purity was measured and confirmed using Nanodrop (Thermo Scientific, Wilmington, DE). Total RNA (385 ng) was reverse transcribed to cDNA templates using MultiScribe reverse transcriptase and random hexamers by incubation at 25 °C for 10 min, followed by reverse transcription at 48 °C for 30 min and enzyme inactivation at 95 °C for 5 min. In all 100 ng of cDNA was amplified by real-time PCR using SYBR Green dye universal master mix on an LightCycler®480 (LC 480) (Applied Biosystems, Inc., Foster City, CA) using the following primers for type 1 collagen (NCBI Accession#; NM_053304.1; forward: TGGTCCCAAAGGTTCTCCTGGT and reverse: TTAGGTCCAGGGAATCCCATCACA), α-SMA (NCBI Accession#; NM_031004.2; forward: ACAACGTGCCTATCTATGAGGGCT and reverse: AGCGACATAGCACAGCTTCTCCTT), TGF-β1 (NCBI Accession#; NM_021578.2; forward: CATCCATGACATGAACCGACCCTT and reverse: ACAGAAGTTGGCATGGTAGCCCTT), TIMP-1 (NCBI Accession#; NM_053819.1; forward: CCTCTGGCATCCTCTTGTTGCTAT and reverse: CATTTCCCACAGCGTCGAATCCTT). The PCR products were subjected to a melting curve analysis and crossing point (Cp) was used for calculating the relative amount of mRNA compared to the house keeping gene, hypoxanthinephophoribosyltransferase (HPRT), and then scaled relative to controls, where control samples were set at a value of 1. Thus, results for all experimental samples were graphed as relative expression compared with the control.

2.8. Histological staining

Formalin-fixed liver specimens from the TFO treated, BDL and Sham operated rats were dehydrated in alcohols, incubated in xylene, and embedded in paraffin. Five-micron-thick tissue sections were cut and stained with either hematoxylin-eosin for general histology or Masson's Trichrome for collagen staining, according to manufacturer's protocols.

2.9. Immunofluorescent staining

Immunofluorescent staining was performed on snap frozen liver tissue. Briefly, 5 μm cryosections were cut on lysine coated slides and fixed in 95% cold ethanol. Slides were air dried and stored at −80 °C till further use. The sections were blocked with 10% goat serum with 1% BSA in PBS for 2 h at room temperature. Cryosections then incubated with the following primary antibodies overnight at 4 °C: anti rabbit α-SMA, anti rabbit TGF-β, and anti-mouse cytoketain-19. The following secondary antibodies were used, anti-rabbit Alexa Fluor 488, anti-mouse Alexa Fluor 594, anti-rabbit Alexa Fluor 594. Nuclear staining was performed using 4′,6-diamidino-2-phenylindole (DAPI). Immunofluorescence was visualized on a Zeiss Apoplan Microscopy system.

2.10. Western blot assay

Proteins were isolated from the liver tissues. The liver tissues were first homogenized and then lysed using 2× Laemmli sodium dodecyl sulfate (SDS) sample buffer containing 100 mM Tris, pH 6.8, 200 mM dithiothreitol (DTT), 4% SDS, 20% glycerol and 0.2% bromophenol blue. The lysate was then boiled for 5 min and subjected to 6% or 10% SDS-polyacrylamide gel electrophoresis (SDS-PAGE) and subsequent transfer to Immobilon polyvinylidene fluoride membrane. After blocking with 5% nonfat dry milk in 1× PBST (PBS containing 0.05% Tween-20) for 1 h at room temperature, the membranes were incubated with rabbit anti type α1(I) collagen and rabbit anti rat TGF-β1 primary antibodies for 16 h at 4 °C. To correct for equal loading and blotting, all blots were re-probed with anti-β-actin antibody. Membrane was then incubated with horseradish peroxidase-conjugated goat anti-rabbit secondary antibody for 1 h at room temperature. Target proteins were detected by enhanced chemiluminescence (ECL) detection kit.

2.11. Myeloperoxidase (MPO) activity assay

The presence of MPO, an enzyme specific for neutrophils, was used as an index of liver neutrophil accumulation as described by Amersi et al. [20]. Briefly, the frozen tissue was thawed and placed in 4 ml iced 0.5% hexadecyl trimethylammonium bromide and 50 mmol potassium phosphate buffer solution with the pH adjusted to 5. Each sample was homogenized for 30 s and centrifuged at 15,000 rpm for 15 min at 4 °C. Supernatants were then mixed with hydrogen peroxide (0.02%), sodium acetate (20 mM) and tetramethyl benzidine (0.15 M) solutions. The change in absorbance was measured spectrophotometrically at 460 nm. One unit of MPO activity was defined as the quantity of enzyme degrading 1 mol peroxide per minute at 25 °C per gram of tissue.

2.12. Statistical analysis

Data are expressed as the mean ± standard deviation (S.D.). Difference between any two groups was determined by ANOVA. $p < 0.05$ was considered statistically significant.

3. Results

3.1. TFO downregulates profibrogenic and proinflammatory cytokines in HSCs in vitro

TGF-β1 and TIMP-1 are the two major profibrogenic cytokines implicated in the development of liver fibrosis [21–23]. As shown in Fig. 1A, transfection of HSC-T6 cells with 1 μg of TFO complexed

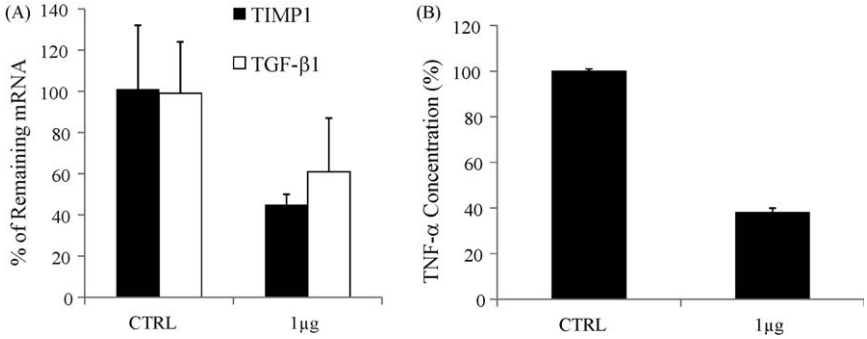

Fig. 1. (A and B) Effect of TFO on TGF-β1, TIMP1 and TNF-α expression after transfection of HSC-T6 cells with TFO after complex formation with Lipofectamine 2000. (A) At 72 h post-transfection, cells were harvested, total RNA was extracted, and TIMP1 and TGF-β1 expression was determined at mRNA levels using real-time PCR. (B) TNF-α concentration in cultured medium was measured by enzyme-linked immunosorbent assay (ELISA).

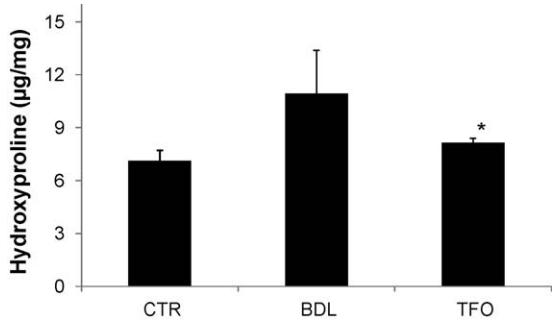

Fig. 2. Effect of TFO treatment on hydroxyproline content in the liver. TFO was injected intravenously at a dose of 8 mg/kg twice a week for 4 consecutive weeks and hydroxyproline content was measured from the liver sections of the control, CBDL and TFO treated rats. Hydroxyproline content was measured by biochemical assay at 7 weeks after BDL. Data are expressed as micrograms of hydroxyproline per milligram of liver tissue. Results are expressed as the mean ± S.D. $^*p < 0.05$ compared to CBDL group using ANOVA. TFO treatment reduces hepatic hydroxyproline content.

with Lipofectamine significantly attenuated expression of TIMP 1 and TGF-β1 mRNAs on real-time PCR. Similarly, TFO significantly decreased proinflammatory cytokine TNF-α concentration in cultured medium as measured by ELISA (Fig. 1B).

3.2. TFO attenuates chronic liver injury in CBDL rats

To examine the effect of TFO on liver fibrosis, the common bile ducts of rats were ligated and at 3 weeks post-CBDL, three rat livers were isolated to confirm liver fibrosis by evaluating (i) macroscopically and (ii) hydroxyproline assay and Masson's trichrome staining for total collagen (data not shown). Then, TFO was injected intravenously twice a week at a dose of 8 mg/kg in the injection volume of 200 μl/rat for 4 consecutive weeks and the degree of liver fibrosis was assessed by using three independent methods: collagen quantitation by measuring hydroxyproline content, Col 1A2 mRNA level in the liver samples and histological analysis by hematoxylin and eosin histological staining as well as Masson Trichrome staining. Hydroxyproline is a quantitative measure of collagen deposition and fibrosis [24]. As expected, there was significant increase in hydroxyproline content in the liver following CBDL, indicating that the liver fibrosis model was successfully established. TFO treatment reduced hydroxyproline content in the fibrotic liver, which was similar to that of the normal rats (Fig. 2).

To determine whether the decrease in hydroxyproline content in the liver of TFO treated CBDL rats was due to the transcription inhibition of α1(1) collagen, we determined collagen gene expression at mRNA and protein levels by real-time PCR and Western blot analysis, respectively. The levels of α1(I) collagen mRNA (corrected by the steady-state levels of HPRT mRNA) were decreased in the liver of TFO treated CBDL rats (Fig. 3A). Similarly, there was significant decrease in the Western blot band thickness of type α1(I) collagen for TFO-treated CBDL rats compared to untreated CBDL rats (Fig. 3B).

3.3. Histopathological alternations

The architecture of fibrotic livers with or without TFO treatment was determined by hematoxylin and eosin histological staining. There was significant number of bile infarcts noticed in the CBDL liver sections (Fig. 4B), but TFO treatment showed significant reduction in the bile infarcts (Fig. 4C). Masson's trichrome staining of the liver sections of the sham, CBDL and TFO-treated CBDL rat livers were also done. In the sham rats which were exposed to saline only, collagen deposition was found surrounding the central veins and enclosing portal triads representing the collagen distribution of healthy livers (Fig. 4D). CBDL rats being treated with saline over 4 weeks displayed a periportal fibrosis characterized by portal-portal septa surrounding the lobules. Collagen deposition was extensive in the peribiliary and interstitial tissue. There were also confluent areas of necrotic hepatocytes in the collagenized zones (Fig. 4E). TFO administration, however, resulted in a marked reduction in the fibrotic stage indicated by decreased portal and periportal accumulation of collagen and essentially no collagen accumulation in the liver interstitium (Fig. 4F).

A computer-aided morphometric analysis revealed that the intensity of collagen staining in the liver sections at 7 weeks after CBDL was reduced by 60% after TFO treatment, when compared with the saline treated CBDL rats.

3.4. Effect of TFO on liver functions and serum fibrotic markers

ALT is a cytosolic enzyme, primarily present in the liver. An increase in plasma ALT indicates liver damage more specifically than AST, which is a mitochondrial enzyme present in large quantities in the heart, liver, skeletal muscle, and kidney, in part indicates liver injury. At 7 weeks post-CBDL, serum AST and ALT levels as determined by colorimetric assay were significantly higher in BDL animals with no TFO treatment compared with the CBDL rats treated with TFO (Fig. 5).

3.5. Effect of TFO on profibrotic genes in vivo

After having shown the suppressive *in vitro* effects of TFO on expression of TGF-β1, a potent profibrogenic cytokine believed to play a central role in regulating tissue fibrosis, we next investigated the effect of TFO on hepatic TGF-β1 expression after CBDL in rats.

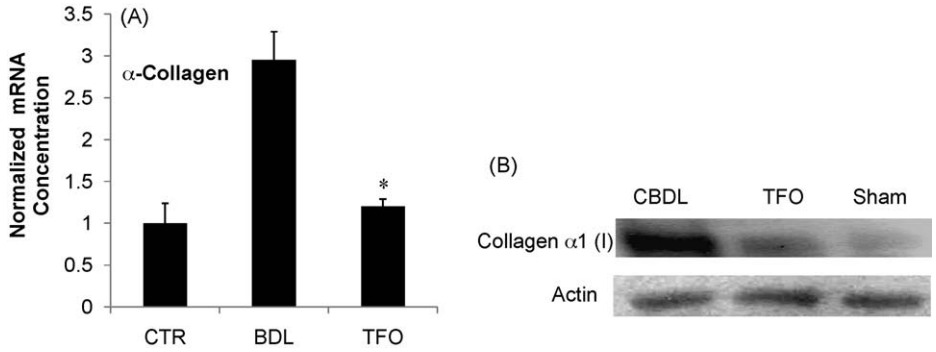

Fig. 3. Effect of TFO treatment on α1(I)-collagen in the liver. (A) RT-PCR and (B) Western blot analysis results showed an inhibitory effect of TFO on α1(I)-collagen expression in the liver at 7 weeks after BDL. RT-PCR results are expressed as the mean ± S.D. $^*p < 0.05$ compared to CBDL group using ANOVA. TFO treatment reduces α1(I)-collagen and α-SMA in the fibrotic liver.

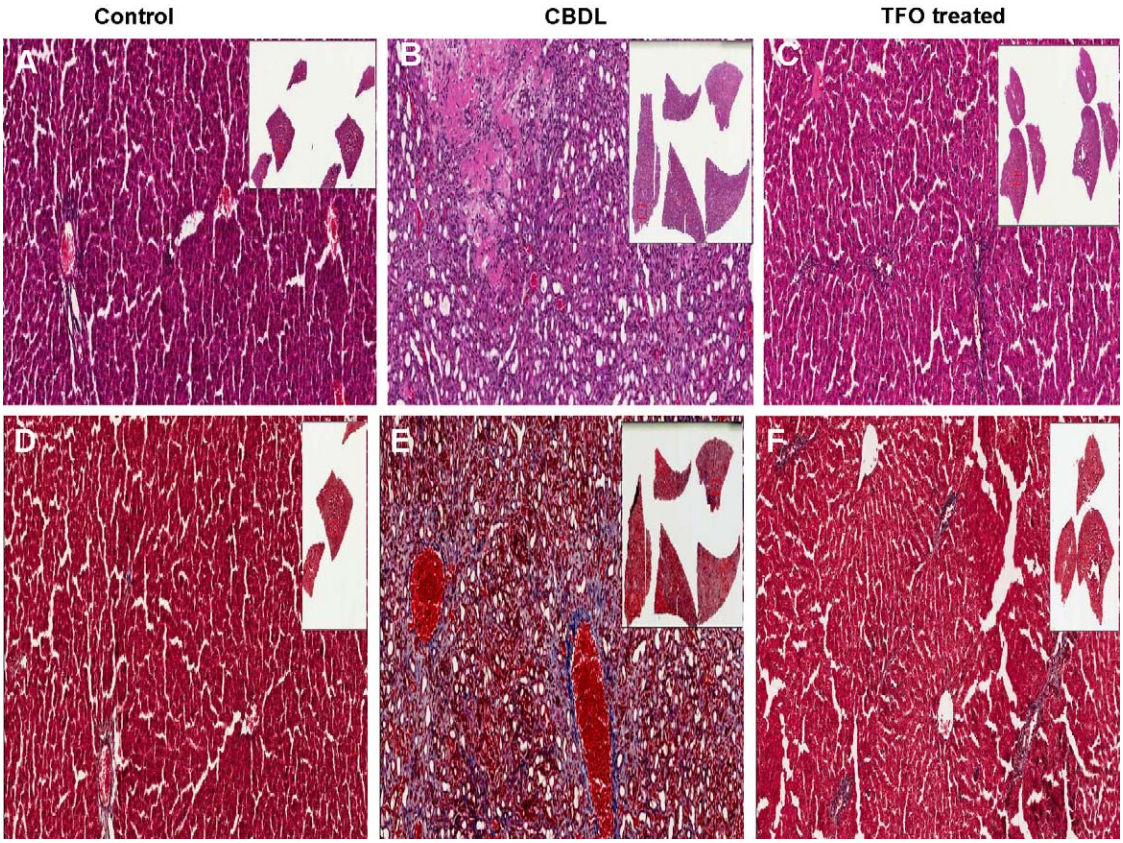

Fig. 4. A TFO treatment attenuates liver fibrosis induced by CBDL. TFO was injected intravenously at a dose of 8 mg/kg twice a week for 4 consecutive weeks and liver tissue sections from the control, BDL and TFO-treated rats were stained with hematoxylin and eosin (A–C), and with Masson's trichrome (D–F) at 7 weeks after BDL. Significantly less hepatic collagen staining was observed in TFO-treated rats.

Western blot analysis of extracted protein samples of the livers showed a strong band for TGF-β1 for CBDL group indicating that CBDL induced a strong upregulation of hepatic TGF-β1 gene expression. In contrast, there was a weak band for TFO treated CBDL and normal rat groups (Fig. 6).

3.6. TFO attenuates in vivo myofibroblast activation

To provide further evidence of the anti-fibrotic properties of TFO in CBDL rats, we used real-time RT-PCR to determine the effects of this compound on hepatic α-SMA protein expression, a well-established marker of HSC activation during liver fibrogenesis [25]. Compared with sham controls, α-SMA mRNA expression in the CBDL liver at 7 weeks was markedly increased (Fig. 7), suggesting the activation of hepatic myofibroblasts following CBDL-induced injury. However, the induction of α-SMA mRNA in the fibrotic liver was largely blocked by intravenous administration of TFO twice a week for four consecutive weeks at 3 weeks after CBDL (Fig. 7).

We next examined hepatic myofibroblast activation after CBDL by using immunofluorescence staining for α-SMA. In the normal rat liver, α-SMA was exclusively and strongly expressed in vessel walls (portal vessels and centrilobular veins) (Fig. 8A). The staining for α-SMA was dramatically increased in CBDL liver forming whorls of layers (onion skinning) around the proliferated bile ductules (Fig. 8B). In addition to the peribiliary region in which α-SMA positive cells were observed, strong α-SMA staining was also found in proliferated biliary epithelia. However, α-SMA staining

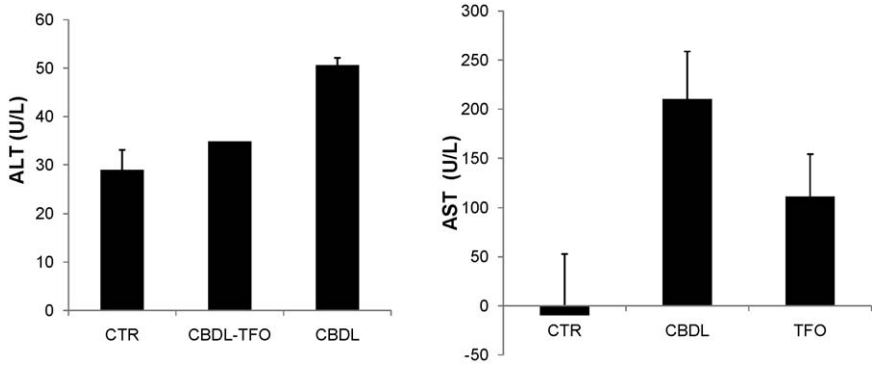

Fig. 5. Effect of TFO treatment on alanine aminotransferase (ALT) and aspartate aminotransferase (AST) content. ALT and AST levels were determined by colorimetric assay at 7 weeks after CBDL in rats. TFO treatment reduces hepatic ALT and AST content compared to CBDL rats without any TFO treatment. Results are expressed as the mean ± S.D.

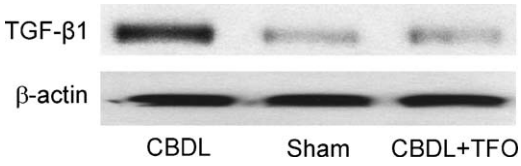

Fig. 6. Effect of TFO on hepatic TGF-β1 in common bile duct ligated (CBDL) rats as determined by Western blot analysis of liver tissues. TGF-β1 concentration was higher for CBDL group, but its level significantly decreased upon TFO treatment.

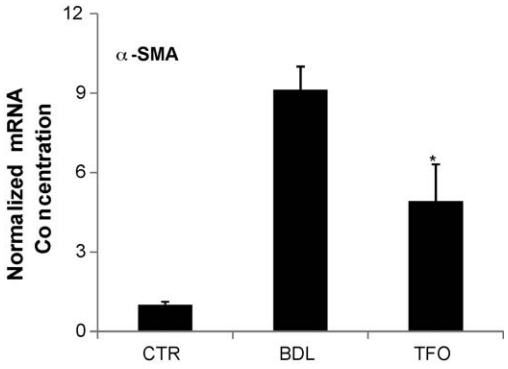

Fig. 7. Effect of TFO treatment on α-SMA in the liver. RT-PCR showed an inhibitory effect of TFO on α-SMA expression in the liver at 7 weeks after BDL. Results are expressed as the mean ± S.D. $^{*}p < 0.05$ compared to CBDL group using ANOVA. TFO treatment reduces α-SMA in the fibrotic liver.

was fairly weak in the fibrotic liver after intravenous administration of TFO twice a week for four consecutive weeks from 3 weeks after CBDL (Fig. 8C).

To confirm the epithelial origin of α-SMA-positive cells, we used double immunofluorescence staining for biliary epithelial marker cytokeratin-19 (red) and α-SMA (green). Clear colocalization (yellow) of cytokeratin-19 and myofibroblast marker α-SMA was seen in biliary epithelial cells at 7 weeks after CBDL (Fig. 9). TFO treatment, however, prevented the coexpression of cytokeratin-19 and α-SMA in biliary epithelium (Figs. 8C and 9F). These observations imply that biliary epithelial cells may undergo a phenotypic transition into myofibroblasts under pathological conditions and that intravenous administration of TFO a week for 4 weeks from the third week after CBDL could protect the biliary epithelia by blocking this phenotypic transition.

3.7. TFO inhibits neutrophil infiltration by downregulating inflammatory cytokines

CBDL may cause hepatocyte apoptosis due to TNF-α upregulation and consequent neutrophil infiltration. Therefore, we determined the amount of TNF-α secreted from the livers of TFO treated and non-treated CBDL rats. There was only slight elevation in TNF-α level in the non-treated CBDL group indicating only minor inflammation following the induction of liver fibrosis by bile duct ligation (Fig. 10A). The level of myeloperoxidase (MPO) which is a marker for neutrophil infiltration was less in the TFO treated CBDL group compared to non-treated CBDL group (Fig. 10B), indicating that TFO treatment can decrease neutrophil infiltration by inhibiting the release of inflammatory cytokine such as TNF-α.

4. Discussion

Fibrosis is characterized by an excessive production of ECM components, especially type I collagen, and if not controlled it can lead to organ dysfunction [26]. Therefore, inhibition of collagen synthesis should prevent fibrosis. Joseph et al. demonstrated that antiparallel polypurine phosphorothioate oligonucleotides could

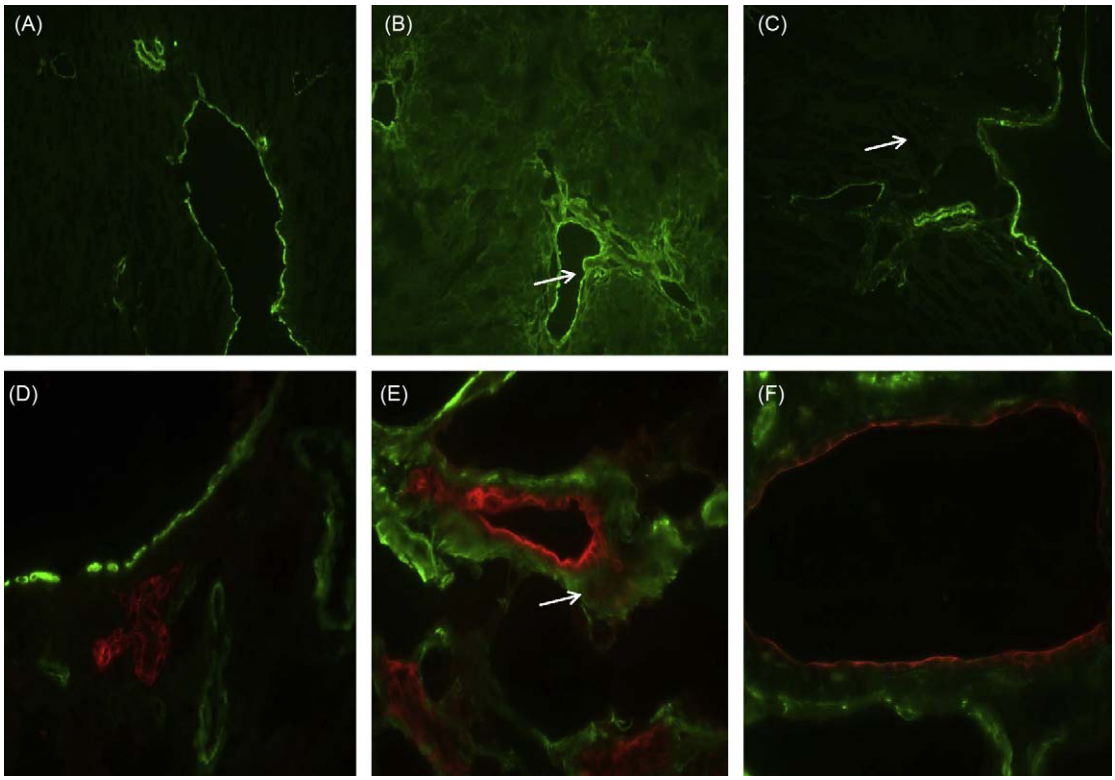

Fig. 8. (A–C) Immunoflorescent staining for α-SMA in (A) Sham, (B) CBDL and (C) TFO treated CBDL-liver sections at 10× magnification, respectively. Arrows indicate the positive staining for α-SMA in and around proliferated bile ductules. (D–F) Double immunostaining for cytokeratin-19 and α-SMA in the sham, CBDL and TFO treated-CBDL liver sections. The arrows indicate the colocalization of cytokeratin-19 and α-SMA indicating the phenomenon of mesenchymal cell transition (EMT) occurring in and around the peribiliary space.

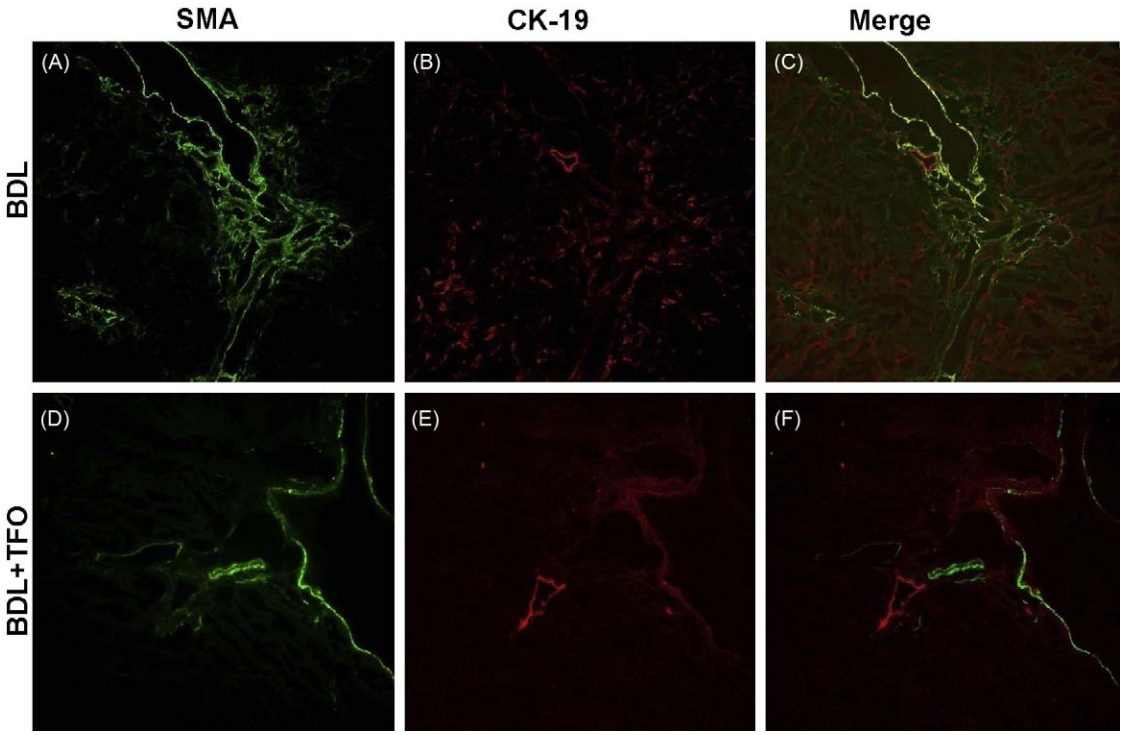

Fig. 9. Double immunostaining for cytokeratin-19 and α-SMA in (A and B) CBDL and (C and D) TFO treated CBDL-liver sections. Merging of cytokeratin-19 and α-SMA is shown in (E) and (F). All the images are at 10× magnification.

form triplexes with the C1 region of the α1(I) collagen gene promoter and inhibit transcription of α1(I) collagen gene promoter activity in rat fibroblasts in culture [27]. We determined triplex formation of a psoralen modified TFO with α1(I) collagen gene in isolated nuclei and intact HSC-T6 cells, and demonstrated strong correlation between triplex formation and transcription inhibition of TFOs [15]. HSCs are the key fibrogenic cells and upon activation they convert into myofibroblast-like cells, excrete excess ECM components, and overexpress TGF-β1 and α-SMA, which are markers for myofibroblasts and fibronectin, respectively [28]. Therefore, in our previous studies, we isolated different liver cells after systemic administration of TFO and demonstrated almost 40% of the total liver recovery was in the HSCs [29].

In the present study, we investigated the therapeutic effect of TFO on liver fibrosis in rats induced by CBDL, which is a commonly used animal model for inducing liver fibrosis. Injury to the bile duct due to ligation results in the formation of α-SMA positive myofibroblasts, which are the major source of type I collagen and fibrogenic cytokines resulting in excessive accumulation of ECM. Hydroxyproline levels in TFO treated CBDL group was markedly decreased as compared to the CBDL group (Fig. 2). This confirms the finding in our previous studies which have suggested that there is also the inhibition of transcription of type I collagen [30].

In liver fibrosis, a combination of collagen deposition in the interstitial matrix and release of proinflammatory cytokines results in diminished blood supply to the biliary ducts leading to biliary infarcts and vanishing bile ducts. Treatment with TFO resulted in reduced activation of HSCs, concentration of fibrogenic mediators (Figs. 6 and 10A) and accumulation of collagen (Figs. 2 and 3). These protective effects were reflected as preserved biliary ducts with lesser biliary infarcts in TFO treated rats, as confirmed by histopathological examination of the liver tissue using Masson's trichrome staining. There was significant decrease in staining for collagen after treatment with TFO twice a week for 4 consecutive

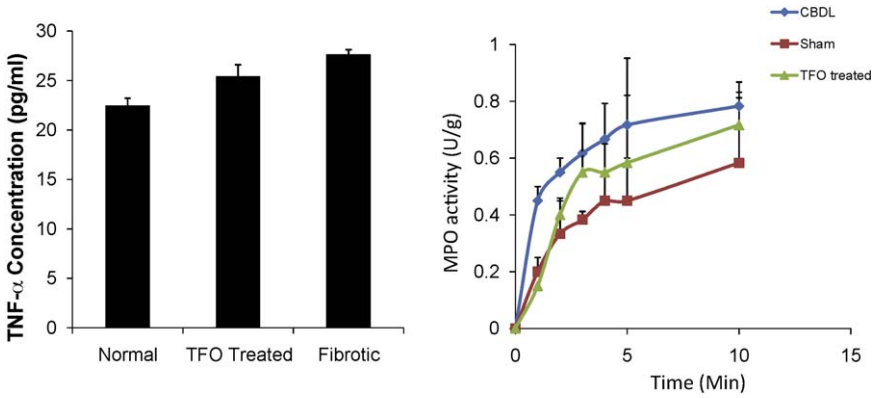

Fig. 10. (A) Effect of *in vivo* TFO treatment on TNF-α. Rat serum was separated from the plasma. Following separation, TNF-α in serum were measured by enzyme-linked immunosorbent assay (ELISA). (B) Myeloperoxidase (MPO) activity in the liver tissue of CBDL, sham and TFO treated groups. One unit of MPO activity was defined as the amount of the MPO in 1 g of liver tissue that could change 1 OD in absorbance at 460 nm.

weeks at 3 weeks post-CBDL (Fig. 4). The increase in concentration of ALT and AST levels seen following CBDL also showed a decreasing trend after TFO treatment (Fig. 5), indicating reduction of hepatic inflammation.

TGF-β1 is also an important factor resulting in EMT resulting in fibrosis. There are several reports in the literature which have showed that TGF-β1 can induce EMT upregulation of Smad-interacting protein-1 (SIP1) and Snail [31–33]. In the present study, TGF-β1 levels were increased significantly following CBDL as seen by Western blot (Fig. 6). Treatment with TFO showed a significant reduction in TGF-β1 levels. These findings suggest that the transformed HSCs may secrete TGF-β1. This is also consistent with the current idea that HSCs are transformed into myofibroblasts and secrete TGF-β1, thus stimulating the production of ECM, and probably their proliferation, through a paracrine/autocrine loop.

In the present study, we have shown that CBDL results in the transformation of BECs to α-SMA expressing myofibroblasts, which migrate into the periductal region through the impaired basement membrane. Most of BECs around the bile duct in CBDL rats were found positive for α-SMA (Fig. 8) corroborating the fact that EMT may be the phenomenon behind the development of myofibroblasts. There was also considerable co-localization of both α-SMA and Cytokeratin-19 in the interstitium around the bile duct suggesting migration of newly formed myofibroblasts (Fig. 9).

TFO treatment can inhibit the transcription of type I collagen and also decrease in α-SMA levels in TFO treated group, suggesting that the inhibition of collagen can also lead to downregulation of α-SMA levels. This helps in attenuating fibrosis induced by CBDL. Furthermore, it also inhibits the EMT, thereby decreasing the development of profibrogenic cells and inhibiting the accumulation of ECM. This study shows that TFO can have a beneficial effect on decreasing liver fibrosis and reversing progression of liver injury. Further studies would be required to understand the exact mechanism by which TFO inhibits EMT.

TFO inhibits the proliferation and type α1(I) collagen production of HSCs. The preservation of liver function is a reflection of the TFO ability to reduce further collagen deposition, which if unchallenged results in further fibrosis and decompensation of liver functions. We further speculate that these beneficial effects may not be seen in already established liver fibrosis reiterating the future need to study its effects on early liver fibrosis.

TNF-α is an important mediator of hepatotoxicity and is upregulated in several animal models of chronic and acute liver injury. Gabele et al have studied the effect of CBDL on TNF-α knockout mice and found them to be more resilient to the liver injury secondary to CBDL [37]. They also showed that TNF-α knockout mice had a significant decrease in expression of collagen, α-SMA and TGF-β1 upon induction of fibrosis by CBDL. In this study, the serum TNF-α levels were elevated following CBDL, and was noted to be lower in the TFO treated group (Fig. 10A). In addition, the TFO treated group also showed less neutrophilic infiltration compared to the CBDL group (Fig. 10B), suggesting the attenuation of liver fibrosis.

Xia et al. have shown that mesenchymal cell transition (EMT) plays a vital role in the development of liver fibrosis due by CBDL [38]. TGF-β1 has also been shown to induce EMT transition to induce idiopathic pulmonary fibrosis [10]. There have been reports, which suggest that the cultured neonatal rat hepatocytes undergo EMT at specific conditions [31]. It will not be surprising if biliary epithelial cells (BECs) undergo phenotypic transition to matrix-producing myofibroblasts after CBDL. It has also been seen that there is a decrease in the hepatic myofibroblast activation and biliary fibrosis when EMT was blocked by hepatocyte growth factor [38].

The principal finding of this study is the antifibrotic effect of TFO, since it decreases the deposition of type α1(I) collagen by reducing the production of collagen, instead of dissolving the collagen. Treatment with TFO was started 3 weeks after the induction of bile duct ligation, which means collagen deposition had already ensued. This collagen was unaffected by TFO treatment suggested by persisting collagen immunostaining seen in the interstitial tissue (Fig. 4F). Albeit the fact that collagen persisted in TFO treated rats, the extent and amount was significantly less than in bile duct ligated control rats (Fig. 4E). Our study further suggests that the treatment of hepatic fibrosis with TFO should begin at the early stage of fibrosis. Our finding is in good agreement with the literature where the inhibitors of type α1(I) collagen synthesis have been shown to reduce the degree of liver injury due to reduced collagen deposition and HSC proliferation [34,35]. Pablo Muriel also demonstrated that significant reduction in the liver collagen deposition and damage induced by prolonged bile duct obstruction in rats after treatment with interferon α [36].

Acknowledgements

The authors wish to thank Dr. Anand Kulkarni, MD, Department of Pathology and Laboratory Medicine for excellent support in microscopy and digitization. This study was supported by a grant from National Institute of Health (to RIM; project number: EB003922).

References

[1] Scott LF. Liver fibrosis – from bench to bedside. J Hepatol 2003;38:38–53.
[2] Bataller R, Brenner DA. Liver fibrosis. J Clin Invest 2005;115:209–18.
[3] Gines P, Cardenas A, Arroyo V, Rodes J. Management of cirrhosis and ascites. N Engl J Med 2004;350:1646–54.
[4] Inagaki Y, Truter S, Greenwel P, Rojkind M, Unoura M, Kobayashi K, et al. Regulation of the [alpha]2(I) collagen gene transcription in fat-storing cells derived from a cirrhotic liver. Hepatology 1995;22:573–9.
[5] Parsons CJ, Takashima M, Rippe RA. Molecular mechanisms of hepatic fibrogenesis. J Gastroenterol Hepatol 2007;22:S79–84.
[6] Arias M, Lahme B, Van de Leur E, Gressner AM, Weiskirchen R. Adenoviral delivery of an antisense RNA complementary to the 3′ coding sequence of transforming growth factor-{beta}1 inhibits fibrogenic activities of hepatic stellate cells. Cell Growth Differ 2002;13:265–73.
[7] Liu C, Gaça MDA, Swenson ES, Vellucci VF, Reiss M, Wells RG. Smads 2 and 3 are differentially activated by transforming growth factor-β (TGF-β) in quiescent and activated hepatic stellate cells. J Biol Chem 2003;278:11721–8.
[8] Marra F, Arrighi MC, Fazi M, Caligiuri A, Pinzani M, Romanelli RG, et al. Extracellular signal-regulated kinase activation differentially regulates platelet-derived growth factor's actions in hepatic stellate cells, and is induced by *in vivo* liver injury in the rat. Hepatology 1999;30:951–8.
[9] Nakatsukasa H, Nagy P, Evarts RP, Hsia CC, Marsden E, Thorgeirsson SS. Cellular distribution of transforming growth factor-beta 1 and procollagen types I, III, and IV transcripts in carbon tetrachloride-induced rat liver fibrosis. J Clin Invest 1990;85:1833–43.
[10] Ramos C, Becerril C, Montano M, Garcia-De-Alba C, Ramirez R, Checa M, et al. FGF-1 reverts epithelial-mesenchymal transition induced by TGF-{beta}1 through MAPK/ERK kinase pathway. Am J Physiol Lung Cell Mol Physiol 2010;299:L222–231.
[11] Soriano V, Labarga P, Ruiz-Sancho A, Garcia-Samaniego J, Barreiro P. Regression of liver fibrosis in hepatitis C virus/HIV-co-infected patients after treatment with pegylated interferon plus ribavirin. AIDS 2006;20:2225–7. doi:10.1097/01.aids.0000247583.38943.95.
[12] Arthur MJP. Reversibility of liver fibrosis and cirrhosis following treatment for hepatitis C. Gastroenterology 2002;122:1525–8.
[13] Knauert MP, Glazer PM. Triplex forming oligonucleotides: sequence-specific tools for gene targeting. Hum Mol Genet 2001;10:2243–51.
[14] Svinarchuk F, Nagibneva I, Cherny D, Ait-Si-Ali S, Pritchard L, Robin P, et al. Recruitment of transcription factors to the target site by triplex-forming oligonucleotides. Nucl Acids Res 1997;25:3459–64.
[15] Ye Z, Guntaka RV, Mahato RI. Sequence-specific triple helix formation with genomic DNA. Biochemistry 2007;46:11240–52.
[16] Xia J-L, Dai C, Michalopoulos GK, Liu Y. Hepatocyte growth factor attenuates liver fibrosis induced by bile duct ligation. Am J Pathol 2006;168:1500–12.
[17] Uchinami H, Seki E, Brenner DA, D'Armiento J. Loss of MMP 13 attenuates murine hepatic injury and fibrosis during cholestasis. Hepatology 2006;44:420–9.
[18] Leonie B, Klaas P, Grietje M, Dirk KFM. Targeting of sugar- and charge-modified albumins to fibrotic rat livers: the accessibility of hepatic cells after chronic bile duct ligation. J Hepatol 1998;29:579–88.

[19] Ramon B, Robert FS, Youkyung HC, Liu Y, Yong Han P, Jeffrey L, et al. NADPH oxidase signal transduces angiotensin II in hepatic stellate cells and is critical in hepatic fibrosis. J Clin Invest 2003;112:1383–94.
[20] Amersi F, Shen XD, Moore C, Melinek J, Busuttil RW, Kupiec-Weglinski JW, et al. Fibronectin-alpha 4 beta 1 integrin-mediated blockade protects genetically fat Zucker rat livers from ischemia/reperfusion injury. Am J Pathol 2003;162:1229–39.
[21] Bissell DM, Roulot D, George J. Transforming growth factor beta and the liver. Hepatology 2001;34:859–67.
[22] Paradis V, Dargere D, Vidaud M, Gouville A-Cd, Huet S, Martinez V, et al. Expression of connective tissue growth factor in experimental rat and human liver fibrosis. Hepatology 1999;30:968–76.
[23] Roderfeld M, Weiskirchen R, Wagner S, Berres M-L, Henkel C, Grotzinger J, et al. Inhibition of hepatic fibrogenesis by matrix metalloproteinase-9 mutants in mice. FASEB J 2006;20:444–54.
[24] Kivirikko KI, Laitinen O, Prockop DJ. Modifications of a specific assay for hydroxyproline in urine. Anal Biochem 1967;19:249–55.
[25] Richard AR, David AB. From quiescence to activation: gene regulation in hepatic stellate cells. Gastroenterology 2004;127:1260–2.
[26] Cheng K, Mahato RI. Gene modulation for treating liver fibrosis. Crit Rev Ther Drug Carrier Syst 2007;24:93–146.
[27] Joseph J, Kandala JC, Veerapanane D, Weber KT, Guntaka RV. Antiparallel polypurine phosphorothioate oligonucleotides form stable triplexes with the rat alpha1(I) collagen gene promoter and inhibit transcription in cultured rat fibroblasts. Nucl Acids Res 1997;25:2182–8.
[28] Honda E, Yoshida K, Munakata H. Transforming growth factor-beta upregulates the expression of integrin and related proteins in MRC-5 human myofibroblasts. Tohoku J Exp Med 2010;220:319–27.
[29] Cheng K, Ye Z, Guntaka RV, Mahato RI. Biodistribution and hepatic uptake of triplex-forming oligonucleotides against type alpha1(I) collagen gene promoter in normal and fibrotic rats. Mol Pharm 2005;2:206–17.
[30] Nakanishi M, Weber KT, Guntaka RV. Triple helix formation with the promoter of human alpha1(I) procollagen gene by an antiparallel triplex-forming oligodeoxyribonucleotide. Nucl Acids Res 1998;26:5218–22.
[31] Kojima T, Takano K, Yamamoto T, Murata M, Son S, Imamura M, et al. Transforming growth factor-beta induces epithelial to mesenchymal transition by down-regulation of claudin-1 expression and the fence function in adult rat hepatocytes. Liver Int 2008;28:534–45.
[32] Caja L, Ortiz C, Bertran E, Murillo MM, Miro-Obradors MJ, Palacios E, et al. Differential intracellular signalling induced by TGF-beta in rat adult hepatocytes and hepatoma cells: implications in liver carcinogenesis. Cell Signal 2007;19:683–94.
[33] Natsuizaka M, Ohashi S, Wong GS, Ahmadi A, Kalman RA, Budo D, et al. Insulin-like growth factor binding protein-3 promotes transforming growth factor-{beta}1-mediated epithelial-to-mesenchymal transition and motility in transformed human esophageal cells. Carcinogenesis 2010;31:1344–53.
[34] Di Sario A, Bendia E, Macarri G, Candelaresi C, Taffetani S, Marzioni M, et al. The anti-fibrotic effect of pirfenidone in rat liver fibrosis is mediated by down-regulation of procollagen alpha1(I), TIMP-1 and MMP-2. Dig Liver Dis 2004;36:744–51.
[35] Pines M, Knopov V, Genina O, Lavelin I, Nagler A. Halofuginone, a specific inhibitor of collagen type I synthesis, prevents dimethylnitrosamine-induced liver cirrhosis. J Hepatol 1997;27:391–8.
[36] Muriel P. Alpha-interferon prevents liver collagen deposition and damage induced by prolonged bile duct obstruction in the rat. J Hepatol 1996;24:614–21.
[37] Gabele E, Froh M, Arteel GE, Uesugi T, Hellerbrand C, Scholmerich J, et al. TNFalpha is required for cholestasis-induced liver fibrosis in the mouse. Biochem Biophys Res Commun 2009;378:348–53.
[38] Xia JL, Dai C, Michalopoulos GK, Liu Y. Hepatocyte growth factor attenuates liver fibrosis induced by bile duct ligation. Am J Pathol 2006;168:1500–12.